Novel Multi-objecitve Evolutionary Algorithm for Color Filter Arrays Design

Lingchen Sun
Northwestern Polytechnical University
Xi'an 710129, China
slcbbd111@sina.com

Lin Li (Corresponding Author)
Northwestern Polytechnical University
Xi'an 710129, China
linli@nwpu.edu.cn

Bin Feng
Northwestern Polytechnical University
Xi'an 710129, China
fengbin@nwpu.edu.cn

Quan Pan
Northwestern Polytechnical University
Xi'an 710129, China
quanpan@nwpu.edu.cn

***Abstract*—Most digital cameras use a single sensor covered with a Color Filter Array (CFA) in order to reduce the size, complexity and cost. Now, more and more researchers have paid attentions to the representation of CFA since its crucial role in the process of reconstructing the full color image. The representation of CFA in frequency domain records all the frequency information of image mosaicked with the CFA, thus provides a theoretical approach to design the CFA. However, almost all the existing CFA design methods in frequency domain have limitations. In this paper, we propose a new automatic CFA design method in frequency domain. We choose the optimal frequency structures which satisfy all the design principles through a novel coded multi-objective evolutionary algorithm (MOEA) at first. Then we convert the parameters optimization of the given frequency structures into a constraint single optimization problem, and we solve it by converting it into a multi-objective optimization problem without constraints which is hard to handle. So a MOEA with novel selection and crossover-mutate strategies is proposed to solve the model. The experimental results show that the proposed CFA design method has more advantage when compared with the other existing method.**

Keywords—Color Filter Array, Evolutionary Algorithm, Discrete Fourier transform, Non-Dominated Sorting

I. INTRODUCTION

Because of the wide use of digital color imaging devices, more and more researchers have paid attention to the process of obtaining an image. In order to reduce the size, complexity and cost, most digital cameras use a single sensor covered with a Color Filter Array(CFA)[2]. A CFA is a physical construction which has the same size as the sensed image and allows only one color component to be sensed at each pixel. The procedure of reconstructing a full color image by estimating the missing two color components in each pixel is called demosaiking[3]. Optimized configurations of CFA can make the subsequent demosaicking process more robust and hence better the quality of the demosaicked images.

Many types of CFA pattern have been proposed including random CFA [4, 5] and irregular CFA [6]. The most common one is the Bayer pattern [7] as shown in Fig.1 (a), which was designed based on the human visual system. From Fig.1 (a), the sampling rates for green, red and blue are 1/2, 1/4 and 1/4, respectively. Based on the Bayer CFA pattern, other CFA patterns have been proposed [8, 9].

(a) Bayer CFA [7] (b) Condat CFA[5] (c) Hirakawa CFA[10]

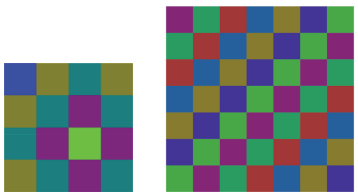

(d) Hao CFA [11] (e) Bai CFA [4]

Fig.1 Five existing CFA patterns .**Images in this paper are best viewed on screen!**

The main shortage of these methods is that the CFAs are represented in spatial domain and it is difficult to search for certain patterns only based on the relationship between the spectral discrete points. To overcome the fundamental limitation of spatial representation, several CFA design methods[4, 11] based on frequency structure were proposed. The frequency structure of the CFA, which records all the information of the mosaicked images at the corresponding frequencies in a matrix, is first calculated and optimized. Then the parameters of the chosen frequency structure are obtained by solving established problem. Full color images with fewer visual artifacts can be produced by these methods based on frequency structure.

However, there are several disadvantages when applying these methods. In [11], the frequency structure is manually specified just with some guidelines and it is difficult to choose

978-1-7281-6929-3/20/$31.00 ©2020 IEEE

appropriate frequency structures for different sizes of arrays without any specific optimization methods. Moreover, in order to optimize the parameters of the chosen frequency structure, a geometric method is employed under certain assumptions. Since the vertices of optimal triangle on the boundary of the feasible region have to be given in advance, the method is difficult to be used when the designed CFA size increases. In [4], an automatic design of CFA method was proposed. The multi-objective evolutionary algorithm (MOEA) is used to obtain the optimal frequency structure and the alternating direction method (ADM) is applied to optimize the parameters of the given frequency structure. In MOEA, three objectives are formulated to be optimized simultaneously, but one objective among three is not conflicted with the other two objectives, which consumes extra amount of computation resource without improving the frequency structure. In addition, they did not consider the redundant nonzero chromas when formulating the optimization objectives. The applied ADM need to update eight parameters per loops which cause it hard to convergence and may make it not be able to obtain the global optimum solution for the parameters of the given frequency structure.

Motivated by the above, this paper proposes a novel automatic CFA design method, which takes all the principles used to design the frequency structure into consideration and is easy to be adapted to different CFA sizes. To obtain the optimal frequency structure, we propose to optimize the two distances (distance between luminance component and chrominance components positions, distance between chrominance components positions) simultaneously through a novel coded MOEA [1, 12, 13]. The individuals are coded in the way that they satisfy the principles of having redundant conjugate and symmetric nonzero chrominance components without locating on the horizontal and vertical axes of luminance component. Then, we model the parameters into a constrained single objective problem. We need to ensure the diversity of solutions in each generation, so a novel MOEA with special strategies based on the nondominated sorting genetic algorithm II (NSGA-II) is used[1], which we will discuss in detail in Section III.

The contributions of the proposed method are:

(1) The proposed CFA design method is automatic.

(2) The proposed models for choosing the frequency structure and optimizing the parameters of the given frequency structure can be solved by using a novel selection and crossover-mutate strategy based on MOEA which could obtain the global optimum solution.

(3) The proposed method can be adopted to design larger sizes of CFA.

In the remainder of this paper, we introduce the frequency structure to represent a CFA filtered image and the CFA design principles in Section II. In Section III, we introduce the proposed CFA design method in detail. In Section IV, we compare the proposed CFA design method with other popular methods. Then, the conclusion and future work are shown in Section V.

II. CFA FREQUENCY PRESENTATION AND DESIGN PRINCIPLES

In this section, we first introduce the frequency presentation of CFA. Then we present the CFA design principles based on frequency structure.

A. Representation of CFA in Frequency Domain

The presentation of CFA is crucial to reconstruct the full color image, however, some existing presentations have limitations. For example, the CFA is represented as discrete points in the spatial domain, which makes it hard to search for certain patterns. Hao[11] proposed using a matrix called frequency structure to record all the frequency information of the mosaicked images. The frequency structure can be easily obtained by computing the symbolic discrete fourier transform(DFT) of the CFA pattern.

Let $f(x,y)$ be the full raw color image with the size of $N_x \times N_y$ and $h_{\mathrm{p}}(x,y)$ be the CFA pattern with the size of $n_{\mathrm{x}} \times n_{\mathrm{y}}$. Both $f(x,y)$ and $h_{\mathrm{p}}(x,y)$ can be decomposed into three components $f^{(\mathrm{C})}(x,y)$ and $h_{\mathrm{p}}{}^{(\mathrm{C})}(x,y)$ based on the established tri-primary color theory, where $\boldsymbol{C} = [R,G,B]^T$.

To ensure the same dynamic range of the sensed image at each pixel, the sum of all primary CFA patterns should be all-one matrix as shown in Eq (1).

$$\sum_{C} h_p^{(C)}(x,y) = 1,\ \forall x,y. \tag{1}$$

Note that CFA pattern is the minimum periodic array since a CFA is usually periodic. Then we can write the CFA as follows.

$$h_{\mathrm{CFA}}^{(C)}(x,y) = h_p^{(C)}\left(x \bmod n_x, y \bmod n_y\right). \tag{2}$$

The CFA filtered image is written as Eq (3).

$$f_{\mathrm{CFA}}(x,y) = \sum_{C} f^{(C)}(x,y) \cdot h_{\mathrm{CFA}}^{(C)}(x,y). \tag{3}$$

Then the DFT of CFA [14] can be formulated as:

$$\begin{aligned} F_{CFA}^{(C)}(\omega_x,\omega_y) &= DFT\left(f^{(C)}(x,y)\cdot h_{CFA}^{(C)}(x,y)\right) \\ &= \sum_{k_x=0}^{n_x-1}\sum_{k_y=0}^{n_y-1} H_p^{(C)}\left(\frac{k_x}{n_x},\frac{k_y}{n_y}\right)\cdot F^{(C)}\left(\omega_x-\frac{k_x}{n_x},\omega_y-\frac{k_y}{n_y}\right) \end{aligned} \tag{4}$$

where $k_{\mathrm{x}} = 0,1,2,...,n_{\mathrm{x}}\text{-}1; k_{\mathrm{y}} = 0,1,2,...,n_{\mathrm{y}}\text{-}1$. Note that $F^{(\mathrm{C})}{}_{\mathrm{CFA}}$ is circularly shifted. Eq (4) implies that the spectrum $F^{(\mathrm{C})}{}_{\mathrm{CFA}}$ is a multiplexing of $n_{\mathrm{x}} \times n_{\mathrm{y}}$ frequency components

centered at $(k_x / n_x, k_y / n_y)$. Then, we compute the spectrum of $h_{CFA}(x,y)$ as Eq (5).

$$\begin{aligned} H_{\mathrm{CFA}}^{(C)}\left(\omega_x,\omega_y\right) &= \mathrm{DFT}\left(h_{\mathrm{CFA}}^{(C)}\left(x,y\right)\right) \\ &= \frac{1}{N_x N_y}\sum_{x=0}^{N_x-1}\sum_{y=0}^{N_y-1} h_{\mathrm{CFA}}^{(C)}\left(x,y\right) e^{-i2\pi\left(\frac{x\omega_x}{N_x}+\frac{y\omega_y}{N_y}\right)} \\ &= \begin{cases} H_p^{(C)}\left(\omega_x,\omega_y\right), \text{if } x\omega_x \in Z \text{ and } y\omega_y \in Z \\ 0 \qquad\qquad\quad , \text{otherwise} \end{cases} \end{aligned} \quad .(5)$$

We record the frequency components in a matrix form by using a matrix $S_{\mathrm{CFA}}^{(C)}$.

$$S_{\mathrm{CFA}}^{(C)} = \left[H_p^{(C)}\left(\frac{k_x}{n_x},\frac{k_y}{n_y}\right)\cdot F^{(C)}\left(\omega\right)\right]_{\substack{k_x=0,1,\cdots,n_x-1 \\ k_y=0,1,\cdots,n_y-1}}. \quad (6)$$

It records all the information of the frequency components in F_{CFA} .Then we can define the frequency structure of a CFA pattern as $S_{\mathrm{CFA}} = \sum_C S_{\mathrm{CFA}}^{(C)}$.

Since $\mathrm{F}^{(C)}(w)$ represents the full raw color image of color C, we can prove that it is a constant term and S_{CFA} is the symbolic DFT of CFA pattern h_p [14].

By applying DFT to Eq (1), Eq (7) can be obtained.

$$\sum_C H_p^{(C)}\left(\frac{k_x}{n_x},\frac{k_y}{n_y}\right) = \delta\left(k_x\right)\delta\left(k_y\right). \quad (7)$$

Eq (7) implies that the sums of coefficients at the baseband (frequency point $(0,0)$) is one and the others are zero. According to [15], we call the multiplex component whose sum is one as luminance component (luma) and the others as chrominance components (chromas).

For example, we can use Eq (4) to compute the frequency structure of Bayer CFA as shown in Fig.1 (a) as Eq (8) shows.

$$S_{Bayer} = \frac{1}{4}\begin{bmatrix} R+2G+B & -R+B \\ R-B & -R+2G-B \end{bmatrix} \quad (8)$$

It records that the frequency component $(R+G+B)/4$ located at frequency point $(0,0)$ is called the luma and the other three components whose location are frequency points $(0.5,0)$, $(0,0.5)$ and $(0.5,0.5)$, respectively are called the chromas. Hence, it can be written as $\begin{bmatrix} F_L & F_{C_2} \\ -F_{C_2} & F_{C_1} \end{bmatrix}$.

B. CFA Design Principles

Since all multiplex components are in the same frequency space, crosstalk can happen in high possibility, thus leading to errors in demosaicking. The spectral characteristics of a CFA can be evaluated by analyzing the degree of the demosaicking errors based on different frequency locations of luma and modulated chromas.

In order to design a CFA with small demosaicking errors, the bandpass filtering will be less likely to aliase from other multiplex components. And, the correlation between multiplex components can be used effectively to improve the accuracy of recovery. Hence, two principles are designed [11]: (P1) The crosstalk among the multiplex components should be as small as possible; (P2) The correlation among some multiplex components should be as high as possible.

According to Eq (8), we can write as follows:

$$\begin{bmatrix} R \\ G \\ B \end{bmatrix} = \boldsymbol{T}^{-1}\begin{bmatrix} F_L \\ F_{C_1} \\ F_{C_2} \end{bmatrix} = \boldsymbol{D}\begin{bmatrix} F_L \\ F_{C_1} \\ F_{C_2} \end{bmatrix}, \quad (9)$$

where $\boldsymbol{D}$ is called demosaicking matrix and $\boldsymbol{T}$ is called transformation matrix. Both the sizes of them are 3×3 . Moreover, we have to reduce the error in the process of estimating multiplex components. According to the linear relationship between the multiplex components, so we can get the third principle for CFA design: (P3) the norm of demosaicking matrix $\boldsymbol{D}$ should be as small as possible.

III. PROPOSED METHOD

Our CFA design method is proposed based on the above three principles. We first choose the optimal frequency structure by satisfying all the principles through a novel coded MOEA. Then we convert the parameters optimization of the given frequency structure into a multi-objective problem without constraints, and we solve it by a MOEA with novel selection and crossover-mutate strategy[16].

A. Modeling the Process of Choosing Frequency Structure:

An appropriate frequency structure should satisfy the principles (P1) and (P2), which means that the location of the multiplex components and the relationship between the chromas need to be specified. Note that the properties of DFT are used to obtain the frequency structure, so S_{CFA} must satisfy all the properties of DFT. Moreover, we take the CFA design principles into consideration. By applying (P1) and (P2), the following four requirements can be obtained:

(G1) To maximize the distance among the nonzero multiplex components;

(G2) The chromas should not locate on the horizontal and vertical axes of luma;

(G3) To minimize the number of the nonzero multiplex components;

(G4) To choose redundant nonzero chromas and make them conjugate symmetry.

Requirement (G1) implies that the distance between luma and chromas and the distance between the chromas should both be as big as possible. Hence, (G1) can be formulated as the following optimization functions $\begin{matrix} f_1 = \max(\min(d_{LC})) \\ f_2 = \max(\min(d_{CC})) \end{matrix}$, where d_{LC} denotes the distance between luma and chromas and d_{CC} denotes the distance between chromas. Note that the frequency structure is periodic in both horizontal and vertical directions. We explain how to calculate the distance by taking the two positions (x_1,y_1) and (x_2,y_2) as an example. The distances along the horizontal and vertical are $d_{\mathrm{x}}=\min(|x_1-x_2|,1-|x_1-x_2|)$ and $d_{\mathrm{y}}=\min(|y_1-y_2|,1-|y_1-y_2|)$ respectively. Hence, the Manhattan distance between the two positions is $d=d_x+d_y$. The multi-objective optimization function in this paper is $\boldsymbol{f}=[f_1,f_2]$.

Now we explain how to satisfy the requirement (G2) by coding the individuals in a population of the evolutionary algorithm. Suppose the size of primary CFA pattern is $n_{\mathrm{x}} \times n_{\mathrm{y}}$. Based on the requirement (G2), the locations of the chromas and luma cannot be on the same horizontal and vertical axes, so the size of input CFA should be $(n_{\mathrm{x}}-1)\times(n_{\mathrm{y}}-1)$.

The requirement (G3) can be written as $\|\boldsymbol{F}\|_0$, where $\boldsymbol{F}$ denotes the multiplex components. (G3) is satisfied by sorting $\|\boldsymbol{F}\|_0$ of all the solutions from Pareto front. In addition, in order to satisfy (G4), we add the redundant nonzero chromas to the optimized results, and make them conjugate symmetry.

It should be noted that the optimal frequency structure cannot be directly obtained. The above model can only filter out most of the bad frequency structures, and the optimal frequency structure need to be chosen through the step of parameter optimization.

We take a 4×4 CFA pattern as an example as shown in Fig.2 (a). Firstly, we input a 3×3 matrix. Secondly, the Pareto front of $\boldsymbol{f}$ is found by an evolutionary algorithm, and the result is shown in Fig.2 (b). The *x*-axis denotes the minimum distance between luma and chromas, the *y*-axis denotes the minimum distance between chromas and the *z*-axis denotes $\|\boldsymbol{F}\|_0$. From Fig.2 (b), the minimum number of multiplex components is 2. Then, three frequency structures are specified by choosing the smallest among the Pareto solutions. Because the chromas are more compact in the frequency domain, chromas are added to the three obtained frequency structures respectively to get final six frequency structures as shown in Fig.2(c).

B. Optimize Parameters

As the frequency structures have been chosen, now we explain how to optimize its parameters. According to [4], the transformation matrix is decomposed into real and imaginary parts, respectively. So the $\boldsymbol{T}$ is expressed as $\boldsymbol{T}^{(1)}+i\boldsymbol{T}^{(2)}$. Hence, Eq (10) is obtained.

$$\begin{bmatrix} F_L \\ F_{C1} \\ F_{C2} \end{bmatrix} = \begin{bmatrix} T_{11}^{(1)}+iT_{11}^{(2)} & T_{12}^{(1)}+iT_{12}^{(2)} & T_{13}^{(1)}+iT_{13}^{(2)} \\ T_{21}^{(1)}+iT_{21}^{(2)} & T_{22}^{(1)}+iT_{22}^{(2)} & T_{23}^{(1)}+iT_{23}^{(2)} \\ T_{31}^{(1)}+iT_{31}^{(2)} & T_{32}^{(1)}+iT_{32}^{(2)} & T_{33}^{(1)}+iT_{33}^{(2)} \end{bmatrix} \begin{bmatrix} R \\ G \\ B \end{bmatrix}. \tag{10}$$

Firstly, we substitute the parameters of $\boldsymbol{T}$ into Eq (10) to get the expression of multiplex components. Secondly, we substitute the multiplex components into the chosen frequency structure. Finally, we calculate the symbolic DFT of it. Then we can obtain the primary CFA pattern h_p with the matrix $\boldsymbol{T}$ as $\boldsymbol{h}_p=\left(\boldsymbol{C}_1\boldsymbol{T}^{(1)}+\boldsymbol{C}_2\boldsymbol{T}^{(2)}\right)\boldsymbol{P}$, where $\boldsymbol{P}$=[R,G,B]$^{\mathrm{T}}$. Let all the parameters of matrix $\boldsymbol{T}^{(1)}$ and $\boldsymbol{T}^{(2)}$ be the matrix of $\boldsymbol{C}_1$ and $\boldsymbol{C}_2$, respectively.

According to the principle (P3) and Eq (1), the following parameter optimization model [11] can be obtained:

$$\begin{aligned} &\min_{\boldsymbol{T}} \left\|\boldsymbol{T}^{-1}\right\|_2 \\ &s.t.\, \boldsymbol{C}_1\boldsymbol{T}^{(1)}+\boldsymbol{C}_2\boldsymbol{T}^{(2)} \geq 0, \left(\boldsymbol{T}^{(1)}+i\boldsymbol{T}^{(2)}\right)\boldsymbol{a}^T=\boldsymbol{e}^T \end{aligned} \tag{11}$$

where $\boldsymbol{T}^{-1}$ is the inverse of $\boldsymbol{T}$, $\mathbf{a}$=[1, 1, 1], $\mathbf{e}$=[1, 0, 0], the range of the elements in $\boldsymbol{T}^{(1)}$ and $\boldsymbol{T}^{(2)}$ is $(-1,1)$.

For optimization problem Eq (11), there are 3 equality constraints and $n_{\mathrm{x}} \times n_{\mathrm{y}}$ inequality constraints. It is quite difficult for traditional mathematical algorithms to deal with. For example, if the CFA is 3×3, the inequality constraints are 9 in total. The more constraints of optimization problem there are, the harder it is to find the satisfied solution. Moreover, the problem Eq (11) is nonconvex which makes it hard to handle. Evolutionary algorithm is suited for solving it.

We need to keep the diversity of the solutions in each generation. Meanwhile, an optimization problem with too many constraints may cause early-maturing in population which means there are too many individuals getting stuck in a local optimum. So there are three main problems we need to solve. The first problem is to deal with the constraints. To keep the diversity of the solutions in each generation is the second problem. And the third problem is to prevent early-maturing in population. Our process of optimizing parameters and the solutions to the above three problems are shown in Fig.3.

We propose to satisfy the equality constraints by coding the individuals and converting the inequality constraints into an objective function, then solve it with a novel selection strategy [16] and a special crossover-mutate strategy based on NSGA-II.

Now we explain how to deal with the equality constraints during coding the individuals in a population. In this paper,

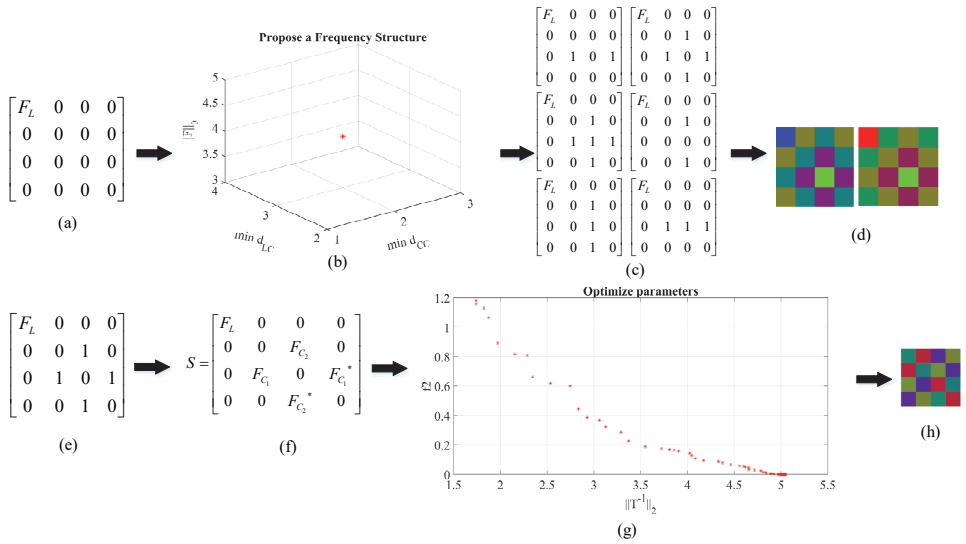

Fig.2 Summary of the proposed CFA design process. From (a) to (h): (a) is the input 4×4 CFA pattern. (b) shows the Pareto front of multi-objective optimization function to choose the optimized chroma positions with the redundant nonzero chromas obtained by our novel coded MOEA, and (c) is the final frequency structures. (d) shows the best performance chroma position obtained from (c). The result of next optimizing the parameters for frequency structure is shown in (g) and finally outputs the obtained CFA (h).

each individual stands for the matrix $\boldsymbol{T}$. We rewrite the equality constraints as follows:

$$\begin{aligned} sum\left(\boldsymbol{T}_{11}+\boldsymbol{T}_{12}+\boldsymbol{T}_{13}\right)&=1\\ sum\left(\boldsymbol{T}_{21}+\boldsymbol{T}_{22}+\boldsymbol{T}_{23}\right)&=0\\ sum\left(\boldsymbol{T}_{31}+\boldsymbol{T}_{32}+\boldsymbol{T}_{33}\right)&=0 \end{aligned}$$

Two 3×3 matrixes stand for $\boldsymbol{T}^{(1)}$ and $\boldsymbol{T}^{(2)}$, whose elements range both from -1 to 1. The first row of $\boldsymbol{T}^{(1)}$ is normalized to satisfy the first equality constraint. Note that luma is conjugated with itself, which means it is a real number with no imaginary. So the elements in the first row of $\boldsymbol{T}^{(1)}$ are non-negative with the range from 0 to 1 and the first row of $\boldsymbol{T}^{(2)}$ is 0. For the second and third equality constraints, we update the last element of the last two rows of $\boldsymbol{T}^{(1)}$ and $\boldsymbol{T}^{(2)}$ as Eq (12) shows.

$$\begin{aligned} \boldsymbol{T}_{23}^{(1)}&=-\left(\boldsymbol{T}_{21}^{(1)}+\boldsymbol{T}_{22}^{(1)}\right)\\ \boldsymbol{T}_{33}^{(1)}&=-\left(\boldsymbol{T}_{31}^{(1)}+\boldsymbol{T}_{32}^{(1)}\right)\\ \boldsymbol{T}_{23}^{(2)}&=-\left(\boldsymbol{T}_{21}^{(2)}+\boldsymbol{T}_{22}^{(2)}\right)\\ \boldsymbol{T}_{33}^{(2)}&=-\left(\boldsymbol{T}_{31}^{(2)}+\boldsymbol{T}_{32}^{(2)}\right) \end{aligned} \tag{12}$$

Let $\boldsymbol{C}_1=\boldsymbol{C}_1^{(1)}+i\boldsymbol{C}_1^{(2)}$ and $\boldsymbol{C}_2=\boldsymbol{C}_2^{(1)}+i\boldsymbol{C}_2^{(2)}$, then inequality constraints can be rewritten as $\boldsymbol{C}_1^{(1)}\boldsymbol{T}_1+\boldsymbol{C}_2^{(1)}\boldsymbol{T}_2\geq\boldsymbol{0},\boldsymbol{C}_1^{(2)}\boldsymbol{T}_1+\boldsymbol{C}_2^{(2)}\boldsymbol{T}_2=\boldsymbol{0}$. Next, we convert it to an objective function as Eq (13) shows.

$$f_2=\begin{cases} -\left(\boldsymbol{C}_1^{(1)}\boldsymbol{T}_1+\boldsymbol{C}_2{}^{(1)}\boldsymbol{T}_2\right) & \boldsymbol{C}_1^{(1)}\boldsymbol{T}_1+\boldsymbol{C}_2{}^{(1)}\boldsymbol{T}_2<\boldsymbol{0}\\ \left|\boldsymbol{C}_1^{(2)}\boldsymbol{T}_1+\boldsymbol{C}_2{}^{(2)}\boldsymbol{T}_2\right| & \boldsymbol{C}_1^{(1)}\boldsymbol{T}_1+\boldsymbol{C}_2{}^{(1)}\boldsymbol{T}_2\geq\boldsymbol{0}\\ & \quad \&\ \&\boldsymbol{C}_1^{(2)}\boldsymbol{T}_1+\boldsymbol{C}_2{}^{(2)}\boldsymbol{T}_2\neq\boldsymbol{0}\\ 0 & \boldsymbol{C}_1^{(1)}\boldsymbol{T}_1+\boldsymbol{C}_2{}^{(1)}\boldsymbol{T}_2\geq\boldsymbol{0}\ \&\ \&\boldsymbol{C}_1^{(2)}\boldsymbol{T}_1+\boldsymbol{C}_2{}^{(2)}\boldsymbol{T}_2=\boldsymbol{0} \end{cases} \tag{13}$$

Hence the parameter optimization problem is modeled as a multi-objective optimized function in $\min_{\boldsymbol{T}}[\left\|\boldsymbol{T}^{-1}\right\|_2, f_2]$.

We only need the individual whose value of f_2 is 0. Hence, we should not pay much attention searching for other individuals whose values of f_2 are nonzero. The information hidden in the other individuals guides the search towards the optimal solution. According to [16], we design $f_{2\max}$ to limit the value of f_2 in each generation. The value of $f_{2\max}$ gets smaller as iterations increases. We delete the individuals whose f_2 value higher than $f_{2\max}$. For the sake of not getting stuck in a local optimum, the value of $f_{2\max}$ cannot be 0, we make the minimum value of $f_{2\max}$ is 1.2.

As the iterations increases, individuals become so similar that it is difficult to reproduce new individuals, thus leading to early-maturing in population. Hence, we delete the individuals with the similar coding before crossover-mutate operator. Moreover, we divide the population into two regions and determine different probability of crossover and mutation to accelerate convergence. The individuals with f_2 value greater than 0.2 are divided into the first region. We determine that the

crossover percentage of first region is lower than the second region, and the mutation percentage is opposite. Given that the overall percentages of crossover and mutation are α and β, the crossover and mutation percentages of first region are α_1 and β_1. We than can calculate two percentages of second region with Eq (14).

$$\begin{aligned}\alpha_2 &= (\alpha \times \mathrm{nPop} - \alpha_1 \times \mathrm{nPop}_1) / \mathrm{nPop}_2 \\ \beta_2 &= (\beta \times \mathrm{nPop} - \beta_1 \times \mathrm{nPop}_1) / \mathrm{nPop}_2,\end{aligned} \tag{14}$$

where nPop, nPop_1 and nPop_2 are the corresponding size of population.

We adopt the simplex crossover (SPX) [17] for its advantages of simplicity and no requirement for information of fitness value. To ensure the diversity of solutions in each generation to obtain global optimization solution, the proposed method is based on NSGA-II.

We optimize the parameters of frequency structure as shown in Fig.2 (e) as an example. The CFA pattern h_P is obtained by calculating the symbolic inverse DFT of the frequency structure. Then we can get $\boldsymbol{C_1}$ and $\boldsymbol{C_2}$ from the expression of h_P as Eq (15) shows.

$$\boldsymbol{C}_1 = \begin{pmatrix} 1 & 2 & 2 \\ 1 & 0 & -2 \\ 1 & -2 & 2 \\ 1 & 0 & -2 \\ 1 & -2 & 0 \\ 1 & 0 & 0 \\ 1 & 2 & 0 \\ 1 & 0 & 0 \\ 1 & 2 & -2 \\ 1 & 0 & 2 \\ 1 & -2 & -2 \\ 1 & 0 & 2 \\ 1 & -2 & 0 \\ 1 & 0 & 0 \\ 1 & 2 & -2 \\ 1 & 0 & 0 \end{pmatrix} \quad \boldsymbol{C}_2 = \begin{pmatrix} i & 0 & 0 \\ i & -2 & 0 \\ i & 0 & 0 \\ i & 2 & 0 \\ i & 0 & -2 \\ i & 2 & 2 \\ i & 0 & -2 \\ i & -2 & 2 \\ i & 0 & 0 \\ i & -2 & 0 \\ i & 0 & 0 \\ i & 2 & 0 \\ i & 0 & 2 \\ i & 2 & -2 \\ i & 0 & 2 \\ i & -2 & -2 \end{pmatrix} \tag{15}$$

Our result is shown in the Fig.2 (g), where *x*-axis represents the norm of $\boldsymbol{T}^{-1}$ and the *y*-axis represents the value of f_2. We can see that the best solution at *x*-axis is 4.96. Note that $f_{2\max}$ limit the non-dominated individual, so there maybe not just one solution that satisfies the constraint. We only need to choose the best solution. The individual with best fitness as shown in Eq (16).

$$\boldsymbol{T} = \begin{bmatrix} 0.3882 & 0.2859 & 0.3258 \\ -0.0803 - 0.0696i & 0.1318 - 0.1079i & -0.0514 - 0.0383i \\ -0.1014 - 0.0977i & -0.0100 - 0.0068i & 0.1114 + 0.1044i \end{bmatrix} \tag{16}$$

The expression of multiplex components are obtained by substituting $\boldsymbol{T}$ into Eq (10). Then the proposed CFA pattern can be obtained by calculating the symbolic inverse DFT of the chosen frequency structure with the proposed the multiplex components. The 4×4 CFA pattern is obtained by the proposed method as shown in Fig.2 (h). We optimize the parameters of the other five frequency structures in Fig.2 (c). And we test their demosaicking performance and choose the best two as shown in Fig.2 (d).

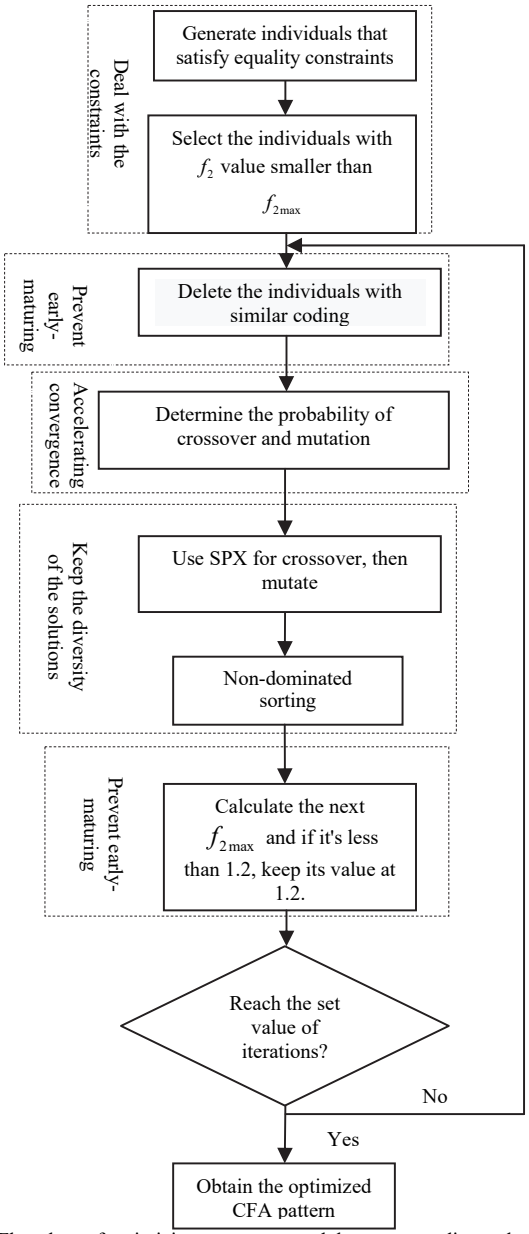

Fig.3 Flowchart of optimizing parameters and the corresponding solutions to the above three problems

IV. EXPERIMENTS

In this section, we validate the effectiveness of the proposed method for CFA design. We test the stability of two proposed algorithms at first. Secondly, we compare the

TABEL III. THE INDIVIDUAL AND AVERAGE CPSNR VALUES

ID	3×2		4×2		4×4		7×7	
	Orig.	*Ours*	*Orig.*	*Ours*	*Orig.*	*Ours*	*Orig.*	*Ours*
1	39.15	39.15	40.16	**40.36**	40.39	40.39	40.99	40.99
2	40.53	40.53	41.19	**41.29**	41.41	41.41	**41.32**	41.30
3	41.91	41.91	42.17	**42.27**	41.13	41.13	**42.69**	42.66
4	40.74	40.74	40.82	**41.13**	41.88	41.88	**40.93**	40.89
5	36.68	36.68	37.09	**37.44**	37.47	37.47	37.94	37.94
6	40.06	40.06	41.39	**41.42**	41.06	41.06	**41.57**	41.54
7	42.23	42.23	42.34	**42.77**	41.64	41.64	**42.20**	42.19
8	37.09	37.09	37.73	**37.83**	37.97	37.97	37.88	37.88
9	42.37	42.37	42.13	**42.47**	41.85	41.85	**42.63**	42.60
10	42.61	42.61	42.52	**42.84**	42.56	42.56	**43.14**	43.11
11	39.97	39.97	**40.47**	40.41	41.01	41.01	40.28	**40.29**
12	43.77	43.77	43.56	**44.23**	43.94	43.94	44.34	**44.39**
13	34.14	34.14	36.71	**37.07**	35.10	35.10	**36.90**	36.89
14	35.97	35.97	**36.60**	36.50	35.80	35.80	36.13	36.13
15	39.67	39.67	39.98	**40.61**	40.44	40.44	40.16	40.19
16	44.32	44.32	45.13	**45.26**	44.42	44.42	**44.97**	44.87
17	40.47	40.47	**41.74**	41.59	41.50	41.50	**41.68**	41.66
18	36.55	36.55	37.38	**37.56**	36.96	36.96	**37.40**	37.39
19	40.75	40.75	**41.56**	41.33	41.41	41.41	**41.57**	41.53
20	40.61	40.61	**41.32**	40.07	40.93	40.93	**41.23**	41.22
21	39.6	39.6	**40.59**	40.50	40.21	40.21	40.22	40.22
22	38.33	38.33	38.36	**38.57**	38.31	38.31	38.60	**38.61**
23	42.65	42.65	42.85	42.85	42.22	42.22	42.64	**42.66**
24	35.03	35.03	**35.88**	35.77	35.42	35.42	35.88	**35.89**
Ave.	39.80	39.80	40.40	**40.51**	40.21	40.21	**40.55**	40.54

performance of CFA patterns designed by our new method with four existing method. They were proposed by Condat [5], Hirakawa [10], Hao [11] and Bai[4].

Our input CFA pattern is set to 4×4 and two algorithms are tested 20 times respectively in order to testify the stability of two proposed algorithm. We use the number of different obtained frequency structure and the norm of demosaicking matrix $\boldsymbol{D}$ as the evaluation indicators of two algorithms respectively. The results are shown in Table I. From Table I, we can get that two variance of results are low. Hence, two algorithms are both stable.

We design four CFAs with the size of 3×2, 4×2, 4×4 and 7×7. And we compare the new CFA patterns with four existing CFAs respectively. For example, the size of the Hirakawa CFA is 4×2 , then our input CFA pattern is set to 4×2 for comparing with it. We design the frequency structure at first, then optimize the parameters to obtain new 4×2 CFA.

We briefly describe the CFA design principles in order to reduce the damosaicking errors caused by crosstalk in subsection II-B. Based on the CFA design principles in subsection II-B, we list characteristics of each CFA in Table II. The characteristics are the minimize distance between luma and chromas, the minimize distance between chromas, the number of nonzero alising components and the norm of the demosaicking matrix. Note that we adapt Euclidean distance to measure the distance.

From the Table II, we can see that the 4×2 CFA designed by the proposed method has the same distance between luma and chromas, distance between chromas, and the number of replicated chromas, but the norm of $\boldsymbol{D}$ is much smaller, which indicates that the error in the process of estimating multiplex components is reduced. Hence, our CFA is better than Hirakawa CFA. The estimation of the color components from the multiplex components can be more accurate with smaller $\|\boldsymbol{D}\|_2$. For 4×4 and 3×2 size, we also design new CFA patterns. But the proposed method does not improve the stability of Hao CFA and Condat CFA. It indicates that global optimization has been achieved. When the size of CFA is small (the size of Hao CFA and Condat CFA are 4×4 and 3×2, respectively), it is easier to obtain the optimal solution through traditional mathematical methods. However, a construction method developed by Condat [5] and the geometric design method used by Hao [18] need to determine the parameters manually and are quite complex in the case of larger input sizes. Compared to Bai CFA with the size of 7×7, our algorithm obtain the higher norm of $\boldsymbol{D}$, but the applied ADM proposed by Bai is hard to convergence and may find the global optimal solutions.

Then we compare the newly designed CFAs with their respective original ones on the Kodak dataset using the same demosaicking algorithm: LSLCD [19]. The individual and average CPSNR values are shown in Table III. The better values in each group are in boldface. From Table III, we can

TABEL I. SUMMARY OF THE EVALUATION INDICATORS OF TWO ALGPTITHM

Algorithm	Choose frequency structure	Optimize paremeters
Best	3	5.6569
Worst	3	5.8336
Average	3	5.6830
Variance	0	5.62×10^{-4}

TABELII. SUMMARY OF THE CHARACTERISTICS OF THE TESTED CFAS

Size	3×2		4×2		4×4		7×7	
	Orig.	*Ours*	*Orig.*	*Ours*	*Orig.*	*Ours*	*Orig.*	*Ours*
Min d_{LC}	0.60	0.60	0.86	0.86	0.75	0.75	0.14	0.14
Min d_{CC}	0.33	0.33	0. 56	0.56	0.25	0.25	0.61	0.61
$\|\|\boldsymbol{F}\|\|_0$	3	3	4	4	5	5	3	3
$\|\|\boldsymbol{D}\|\|_2$	3.00	3.00	4.24	**4.03**	5.66	5.66	**3.33**	3.35

see that our newly designed CFAs have identical CPSNR with Condat CFA and Hao CFA, respectively. The proposed 4×2 CFA has better performance than Hirakawa CFA which is same as the analysis as above. Compared with Bai CFA, the results of the proposed CFA still have better performance in some data but the average rsults is worse than Bai CFA.

V. CONCLUSION

In this paper, We propose a novel automatic CFA design method in frequency domain, which can satisfy all the frequency design principles. The proposed models for choosing the frequency structure and optimizing the parameters of the given frequency structure can be solved by using a novel strategy based on MOEA which could obtain the global optimum solution. The proposed method can be adopted to design larger sizes of CFA in less amount of computation. The experimental results show that the proposed CFA design method is more advantage when compared with the other existing method. However we find that the CFA meeting all the design principles could not make all the test data reach the optimal value during the experiment. Our future work will focus on the improvement of CFA design principles in frequency domain.

ACKNOWLEDGMENT

This research work was supported by the Fundamental Research Funds for the Central Universities (3102019ZDHKY08).

REFERENCES

[1] K. Deb, A. Pratap, S. Agarwal, and T. Meyarivan, "A fast and elitist multiobjective genetic algorithm: NSGA-II," *IEEE transactions on evolutionary computation,* vol. 6, no. 2, pp. 182-197, 2002.

[2] J. Adams, K. Parulski, and K. Spaulding, "Color processing in digital cameras," *IEEE micro,* vol. 18, no. 6, pp. 20-30, 1998.

[3] D. Menon and G. Calvagno, "Color image demosaicking: An overview," *Signal Processing Image Communication,* vol. 26, no. 8, pp. 518-533, 2011.

[4] C. Bai, J. Li, Z. Lin, and J. Yu, "Automatic Design of Color Filter Arrays in The Frequency Domain," *IEEE Transactions on Image Processing A Publication of the IEEE Signal Processing Society,* vol. 25, no. 4, pp. 1793-1807, 2016.

[5] L. J. I. Condat and V. Computing, "Color filter array design using random patterns with blue noise chromatic spectra," *Image and Vision Computing,* vol. 28, no. 8, pp. 1196-1202, 2010.

[6] C. Bai, J. Li, Z. Lin, J. Yu, and Y. W. Chen, "Penrose Demosaicking," *IEEE Trans Image Process,* vol. 24, no. 5, pp. 1672-1684, 2015.

[7] B. E. Bayer, "Color imaging array," ed: Google Patents, 1976.

[8] T. Yamagami, T. Sasaki, A. Suga, and C. K. Kaisha, "Image signal processing apparatus having a color filter with offset luminance filter elements," in *Us Patent*, 1994.

[9] K. Hirakawa and P. J. Wolfe, "Spatio-Spectral Color Filter Array Design for Optimal Image Recovery," *IEEE Transactions on Image Processing A Publication of the IEEE Signal Processing Society,* vol. 17, no. 10, pp. 1876-90, 2008.

[10] K. Hirakawa and P. J. Wolfe, "Spatio-spectral color filter array design for optimal image recovery," *IEEE Transactions on Image Processing,* vol. 17, no. 10, pp. 1876-1890, 2008.

[11] P. Hao, Y. Li, Z. Lin, and E. Dubois, "A geometric method for optimal design of color filter arrays," *IEEE Transactions on Image Processing A Publication of the IEEE Signal Processing Society,* vol. 20, no. 3, pp. 709-22, 2011.

[12] L. Li, X. Yao, R. Stolkin, M. Gong, and S. He, "An evolutionary multiobjective approach to sparse reconstruction," *IEEE Transactions on Evolutionary Computation,* vol. 18, no. 6, pp. 827-845, 2014.

[13] L. Li, L. Jiao, R. Stolkin, and F. Liu, "Mixed second order partial derivatives decomposition method for large scale optimization," *Applied Soft Computing,* vol. 61, pp. 1013-1021, 2017.

[14] Y. Li, P. Hao, and Z. Lin, "The frequency structure matrix: A representation of color filter arrays," *International Journal of Imaging Systems & Technology,* vol. 21, no. 1, pp. 101-106, 2015.

[15] A. David, S. Sabine, and H. Jeanny, "Linear demosaicing inspired by the human visual system," *IEEE Transactions on Image Processing,* vol. 14, no. 4, pp. 439-449, 2005.

[16] L. Jiao, L. Li, R. Shang, F. Liu, and R. Stolkin, "A novel selection evolutionary strategy for constrained optimization," *Information Sciences,* vol. 239, pp. 122-141, 2013.

[17] T. Higuchi, S. Tsutsui, and M. Yamamura, "Theoretical analysis of simplex crossover for real-coded genetic algorithms," in *International Conference on Parallel Problem Solving from Nature*, 2000, pp. 365-374: Springer.

[18] H. Pengwei, L. Yan, L. Zhouchen, and D. Eric, "A geometric method for optimal design of color filter arrays," *IEEE Transactions on Image Processing A Publication of the IEEE Signal Processing Society,* vol. 20, no. 3, pp. 709-22, 2011.

[19] B. Leung, G. Jeon, and E. Dubois, "Least-Squares Luma–Chroma Demultiplexing Algorithm for Bayer Demosaicking," *IEEE Transactions on Image Processing,* vol. 20, no. 7, pp. 1885-1894, 2011.